

Supplementary Materials for

Nuclear HMGB1 protects from nonalcoholic fatty liver disease through negative regulation of liver X receptor

Jean Personnaz, Enzo Piccolo, Alizée Dortignac, Jason S. Iacovoni, Jérôme Mariette, Vincent Rocher, Arnaud Polizzi, Aurélie Batut, Simon Deleruyelle, Lucas Bourdens, Océane Delos, Lucie Combes-Soia, Romain Paccoud, Elsa Moreau, Frédéric Martins, Thomas Clouaire, Fadila Benhamed, Alexandra Montagner, Walter Wahli, Robert F. Schwabe, Armelle Yart, Isabelle Castan-Laurell, Justine Bertrand-Michel, Odile Burlet-Schiltz, Catherine Postic, Pierre-Damien Denechaud, Cédric Moro, Gaëlle Legube, Chih-Hao Lee, Hervé Guillou, Philippe Valet, Cédric Dray, Jean-Philippe Pradère*

*Corresponding author. Email: jean-philippe.pradere@inserm.fr

Published 25 March 2022, *Sci. Adv.* **8**, eabg9055 (2022)
DOI: [10.1126/sciadv.abg9055](https://doi.org/10.1126/sciadv.abg9055)

This PDF file includes:

Figs. S1 to S11
Tables S1 to S3

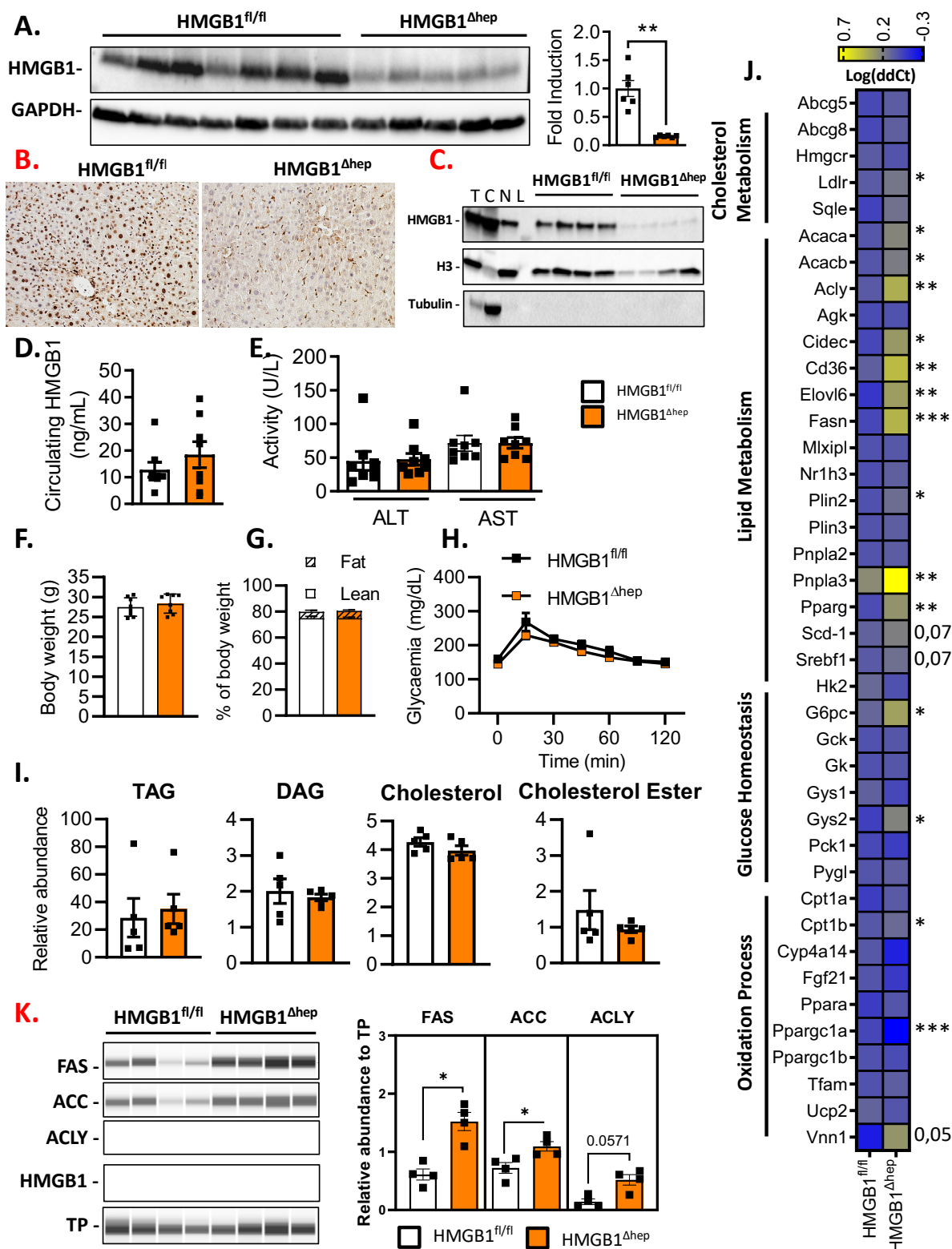


Fig. S1. Metabolic explorations of Hepatocyte specific *Hmgb1* deleted mice subjected to chow-diet.

(A) Representative immunoblot targeting HMGB1. GAPDH was used as a loading control. Densitometric quantification (right panel) performed on the whole animal cohort, on liver biopsies from on 8 week-old $\text{HMGB1}^{\text{fl/fl}}$ ($n=7$) and $\text{HMGB1}^{\Delta\text{Hep}}$ ($n=5$) mice fed on chow diet. (B) HMGB1 staining determined by IHC on liver sections and (C) immunoblot targeting HMGB1 on nuclear extracts in livers from $\text{HMGB1}^{\text{fl/fl}}$ and $\text{HMGB1}^{\Delta\text{Hep}}$ mice fed on chow diet (C). Histone 3 (H3) was used as a nuclear marker while Tubulin was used as a cytoplasm marker and control lanes as follow: T= total lysates, C=Cytoplasm extracts, N=Nucleus extracts and L=ladder. (D-E) Circulating levels of HMGB1 (D) and hepatic transaminases (E), (F) Body weight, (G) percentage of lean and fat mass, (H) analysis of oral glucose tolerance test and (I) liver neutral lipid levels in liver sections of 8 week-old $\text{HMGB1}^{\text{fl/fl}}$ and $\text{HMGB1}^{\Delta\text{Hep}}$ mice fed on chow diet. (J) Heatmap showing gene expression of specific markers involved in hepatic lipid and glucose metabolism determined by microfluidic RT-qPCR. (K) Immunoblot targeting key lipogenic enzymes FAS, ACC, ACLY and HMGB1 was performed on liver biopsies from on 12 week-old $\text{HMGB1}^{\text{fl/fl}}$ ($n=4$) and $\text{HMGB1}^{\Delta\text{Hep}}$ ($n=4$) mice fed on chow diet and densitometric quantification (right panel) normalized by the total protein load (TP). Data are means \pm SEM of three independent experiments. * $p<0.05$, ** $p<0.01$, *** $p<0.001$, **** $p<0.0001$ by unpaired Mann and Whitney comparison

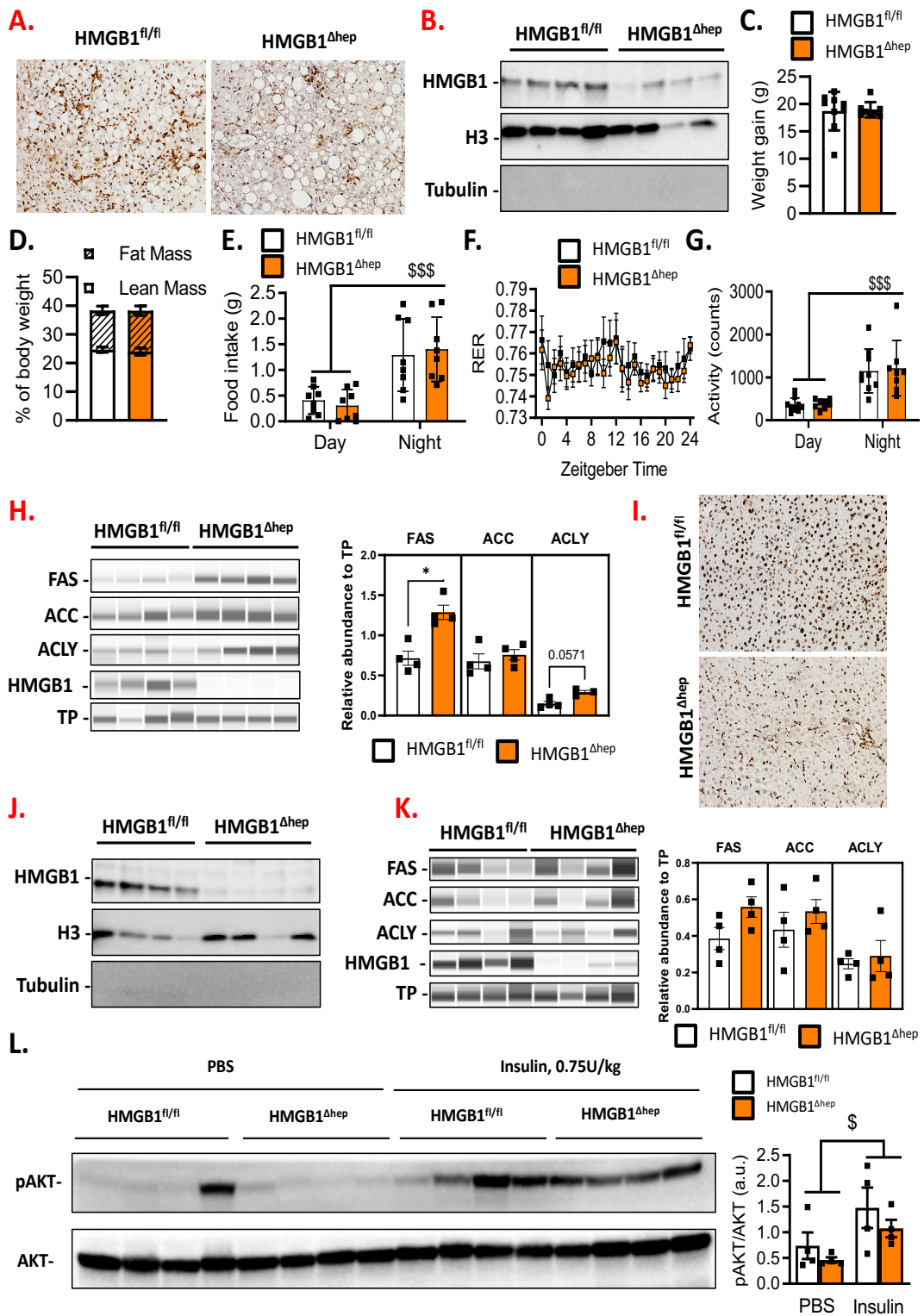


Fig. S2. Metabolic explorations of Hepatocyte specific *Hmgb1* deleted mice subjected to high-fat diet and F/R.

(A-B) HMGB1 staining determined by IHC on liver section (A) and immunoblot targeting HMGB1 on nuclear extracts from livers of HMGB1^{fl/fl} and HMGB1^{ΔHep} mice fed on 12 week-high-fat diet. Histone 3 (H3) was used as a nuclear marker while Tubulin was used as a cytoplasm marker (B). (C) Weight gain and (D) body fat and lean mass of HMGB1^{fl/fl} (n=9) and HMGB1^{ΔHep} (n=8) mice on HFD. (E-G) Indirect calorimetry analysis monitoring (E) food intake, (F) Respiratory exchange Ratio (RER) and (G) spontaneous physical activity of HMGB1^{fl/fl} (n=8) and HMGB1^{ΔHep} (n=8) mice on HFD during 24 hours. (H) Immunoblot targeting key lipogenic enzymes FAS, ACC, ACLY and HMGB1 was performed on liver biopsies from HMGB1^{fl/fl} (n=4) and HMGB1^{ΔHep} (n=4) mice fed subjected to 12 week-HFD60% and densitometric quantification (right panel) normalized by the total protein load (TP). (I-J) HMGB1 staining determined by IHC on liver section (I) and immunoblot targeting HMGB1 on nuclear extracts from livers of HMGB1^{fl/fl} and HMGB1^{ΔHep} mice after F/r challenge (J). (K) Immunoblot targeting key lipogenic enzymes FAS, ACC, ACLY and HMGB1 was performed on liver biopsies from on 8 week-old HMGB1^{fl/fl} (n=4) and HMGB1^{ΔHep} (n=4) mice after F/R challenge and densitometric quantification (right panel) normalized by the total protein load (TP). (L) Representative immunoblot targeting p-AKT and Tot-AKT was used as a loading control. Densitometric quantification (right panel) performed on the whole animal cohort, on liver biopsies from on 8 week-old HMGB1^{fl/fl} and HMGB1^{ΔHep} mice fed on chow diet and challenged with an acute injection of PBS (100uL) (n=4 for each genotype) or insulin (i.p, 0.75 U/kg) (n=4 for each genotype). Livers were harvested 15 minutes after insulin stimulation. Data are means ± SEM of three independent experiments. *p<0.05, **p<0.01, ***p<0.001, ****p<0.0001 by unpaired Mann and Whitney comparison or two-way ANOVA. \$ p<0.05, \$\$ p<0.01, \$\$\$ p<0.001, for treatment effect by two-way ANOVA.

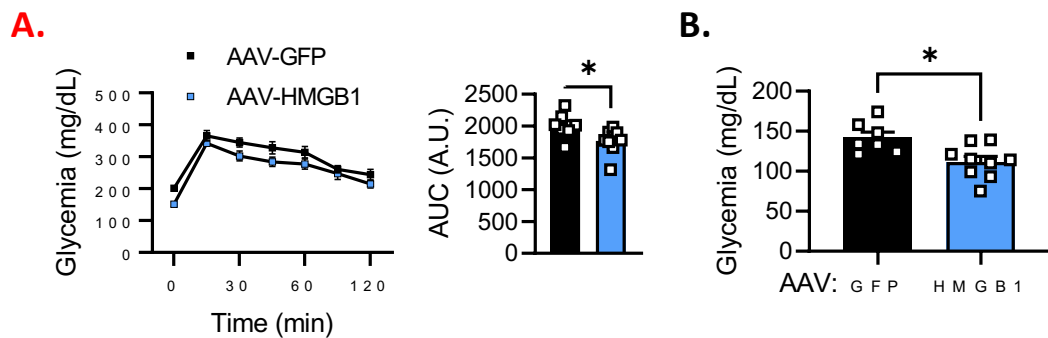


Fig. S3. Hepatic overexpression of HMGB1 improves glucose homeostasis.

(A) Analysis of oral glucose tolerance test with AUC representation and (B) fasting glycemia levels after overnight fasting. Data are means \pm SEM of three independent experiments. * $p<0.05$, by unpaired Mann and Whitney comparison

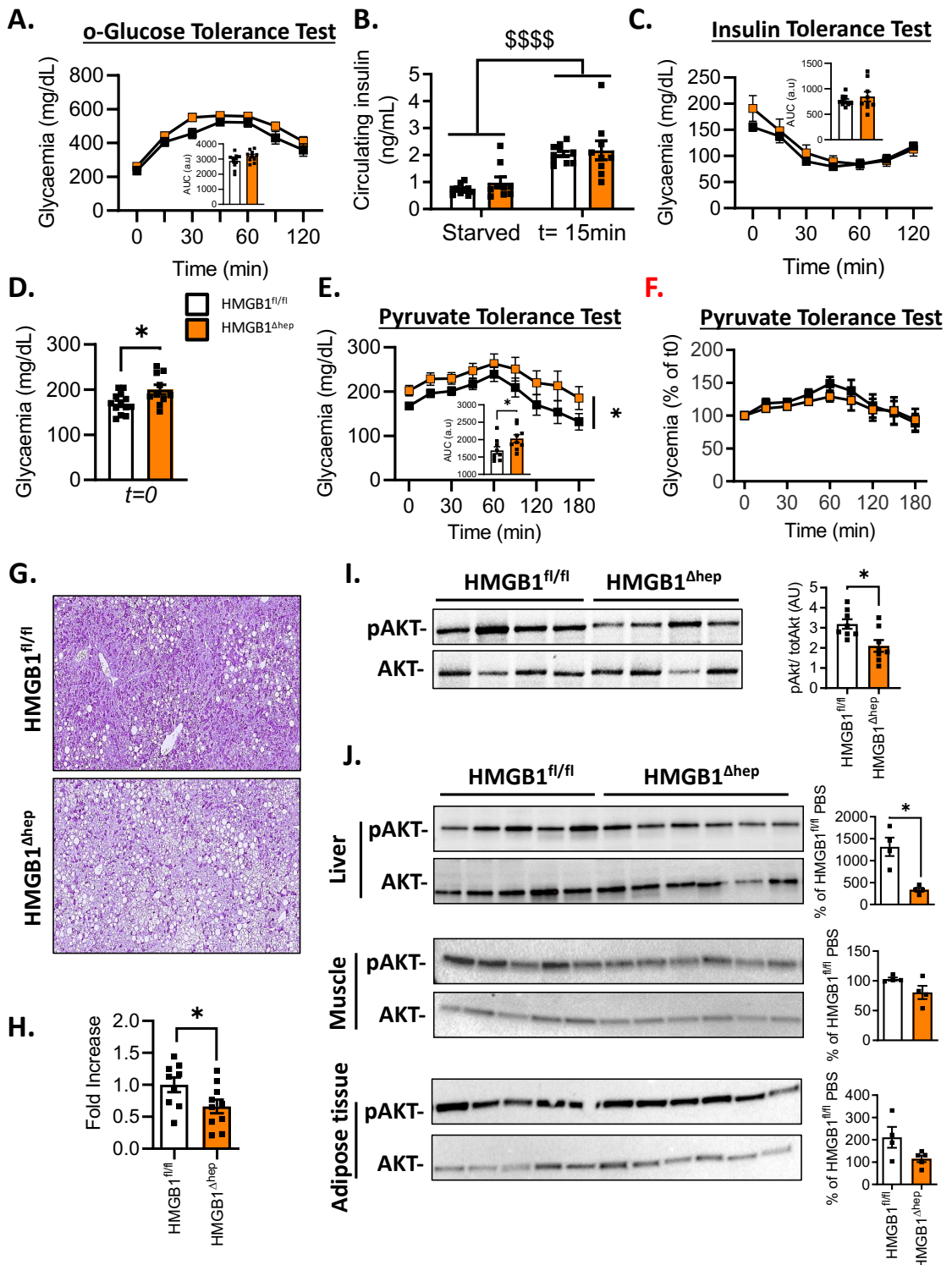


Fig. S4. Hepatocyte specific *Hmgb1* deleted mice on HFD display reduced insulin sensitivity in the liver.

(A) Analysis of oral glucose tolerance test, (B) Insulin levels after fasting or 15 minutes post glucose bolus, (C) insulin tolerance test, (D) fasting glycaemia levels after 16 hours of fasting and (E-F) pyruvate tolerance test on HMGB1^{fl/fl} and HMGB1^{ΔHep} mice fed on HFD for 12 weeks expressed with absolute values (E) or percentage from the baseline (F). (G-H) Hepatic PAS staining representative images with (H) quantification on HMGB1^{fl/fl} and HMGB1^{ΔHep} mice fed on HFD for 12 weeks. (I) Representative immunoblot targeting p-AKT and tot-AKT with quantification performed on the whole animal cohort, on liver biopsies from on HMGB1^{fl/fl} and HMGB1^{ΔHep} mice fed on HFD for 12 weeks. (J) Representative immunoblot targeting p-AKT and tot-AKT with quantification performed on the whole animal cohort, on liver, skeletal muscle (gastrocnemius) and adipose tissue (perigonadal fat pad noted PG) biopsies from HMGB1^{fl/fl} and HMGB1^{ΔHep} mice fed on HFD for 24 weeks, starved 4 hours and injected with insulin (i.p. 0.75U/kg-15 minutes). Data are means ± SEM from n=10 (HMGB1^{fl/fl}) or n=11 (HMGB1^{ΔHep}) per group for the HFD protocol (A-H) and from n=4 (HMGB1^{fl/fl}) or n=4 (HMGB1^{ΔHep}) per group for the HFD 24-week with acute injection of insulin protocol (J). *p<0.05, **p<0.01, ***p<0.001, ****p<0,0001 by unpaired Mann and Whitney comparison or two-way ANOVA.

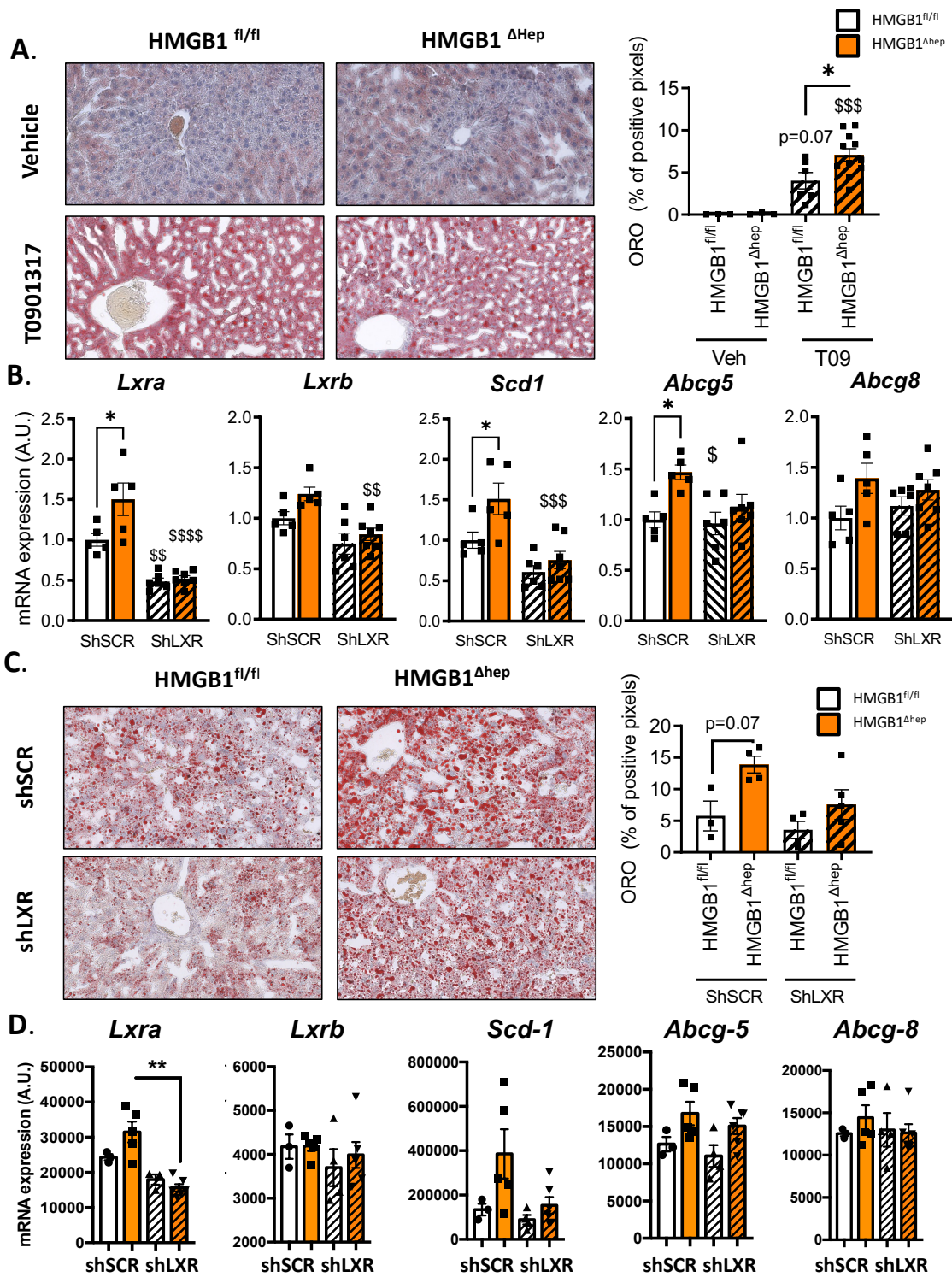


Fig. S5. Hepatocyte specific *Hmgb1* deleted mice exhibit a severe liver steatosis under metabolic stress that is restored by knocking-down LXRA *in vivo*.

(A) 8 week-old HMGB1^{fl/fl} (n=5) and HMGB1^{ΔHep} (n=9) mice fed on chow diet were treated either with vehicle (5% carboxy-methyl-cellulose) (HMGB1^{fl/fl} (n=5) and HMGB1^{ΔHep} (n=3)) or LXRA synthetic agonist T0901317 (oral gavage, 30 mg/kg/day) (HMGB1^{fl/fl} (n=10) and HMGB1^{ΔHep} (n=7)) for four consecutive days, after 6 hours starvation on the last day mice were sacrificed. (A) Liver steatosis was assessed by Oil Red-O staining on liver sections with the quantitative representation displayed on the right. (B) HMGB1^{fl/fl} and HMGB1^{ΔHep} mice were infected with either adenovirus expressing a scramble (shSCR, HMGB1^{fl/fl}, n=6 and HMGB1^{ΔHep}, n=7) or an LXRA shRNA (shLXR, HMGB1^{fl/fl}, n=5 and HMGB1^{ΔHep}, n=5) sequence, then subjected 7 days later to a F/R challenge was then subjected to RT-qPCR analysis of the indicated LXRA dependent genes. (C-D) HMGB1^{fl/fl} and HMGB1^{ΔHep} mice were subjected to HFD for four weeks and then infected with either adenovirus expressing a scramble (shSCR, HMGB1^{fl/fl}, n=2 and HMGB1^{ΔHep}, n=5) or an Lxra shRNA (shLxra, HMGB1^{fl/fl}, n=4 and HMGB1^{ΔHep}, n=6) sequence and euthanized 7 days later. Liver steatosis was determined by quantifying Oil Red-O staining (C) and shLxra efficiency was assessed by measuring indicated LXRA dependent gene expression using RT-qPCR (D). Data are means ± SEM. *p<0.05, **p<0.01, ***p<0.001, ****p<0.0001 for HMGB1^{fl/fl} and HMGB1^{ΔHep} comparison, by unpaired Mann and Whitney comparison. \$ p<0.05, \$\$ p<0.01, \$\$\$ p<0.001, for treatment effect by one-way ANOVA.

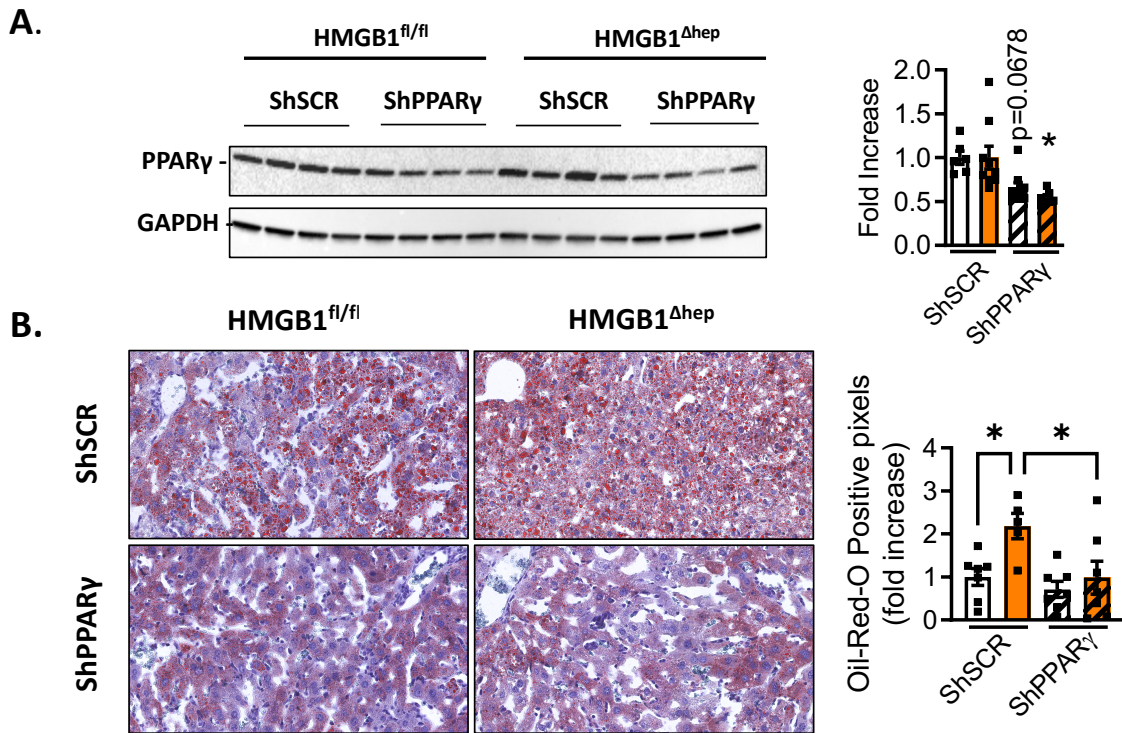


Fig. S6. Hepatocyte specific *Hmgb1* deleted mice exhibit a severe liver steatosis under metabolic stress that is restored by knocking-down PPAR γ *in vivo*.

(A) Immunoblot targeting PPAR γ , with GAPDH used as a loading control. (B) HMGB1 $^{\text{fl}/\text{fl}}$ and HMGB1 $^{\Delta\text{Hep}}$ mice were subjected to HFD for four weeks and then infected with either adenovirus expressing a PPAR γ shRNA (shPPAR γ , HMGB1 $^{\text{fl}/\text{fl}}$, n=7 and HMGB1 $^{\Delta\text{Hep}}$, n=7) or a scramble (shSCR, HMGB1 $^{\text{fl}/\text{fl}}$, n=7 and HMGB1 $^{\Delta\text{Hep}}$, n=5) sequence and euthanized 7 days later. Liver steatosis was assessed by Oil Red-O staining on liver section tissue with the quantitative representation displayed on the right. *p<0.05, **p<0.01, ***p<0.001, ****p<0.0001 for HMGB1 $^{\text{fl}/\text{fl}}$ and HMGB1 $^{\Delta\text{Hep}}$ comparison, by unpaired Mann and Whitney comparison or by one-way ANOVA.

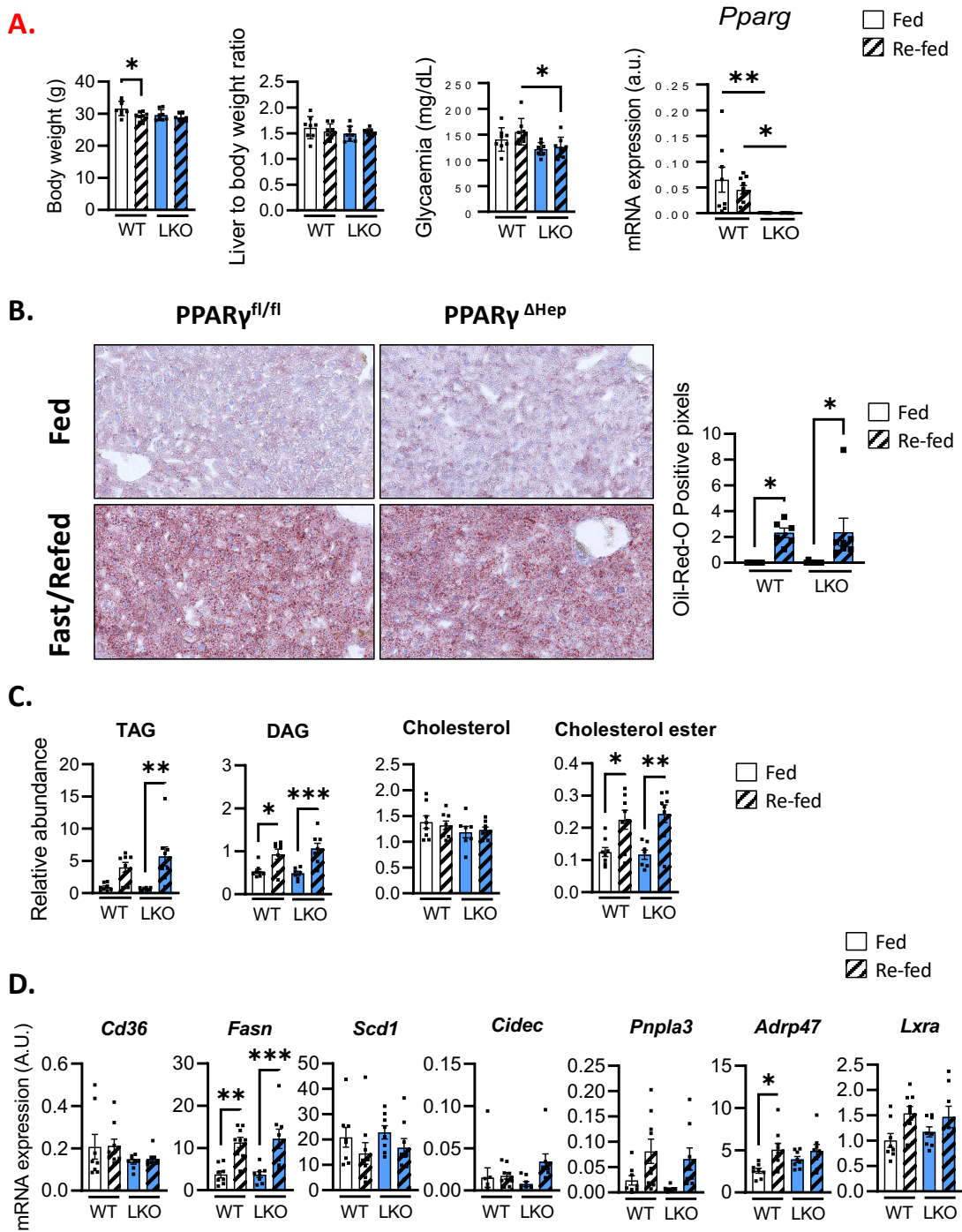


Fig. S7. Hepatocyte specific *Ppary* deletion does not modify liver steatosis in mice after F/R challenge.

PPAR $\gamma^{fl/fl}$ and PPAR $\gamma^{\Delta Hep}$ ($n=8$) mice were subjected to F/R challenge. (A) Body weight, liver/body weight ratio and starved glycaemia of mice on fed (6 hours)-refeed (8 hours). Hepatic steatosis was assessed by (B) Oil Red-O staining with quantification (right panel) and (C) neutral lipids analysis. (D) mRNA expression of hepatic steatosis markers from liver biopsies was determined by RT-qPCR. Data are means \pm SEM of three independent experiments. * $p<0.05$, ** $p<0.01$, *** $p<0.001$, **** $p<0.0001$ by unpaired Mann and Whitney comparison.

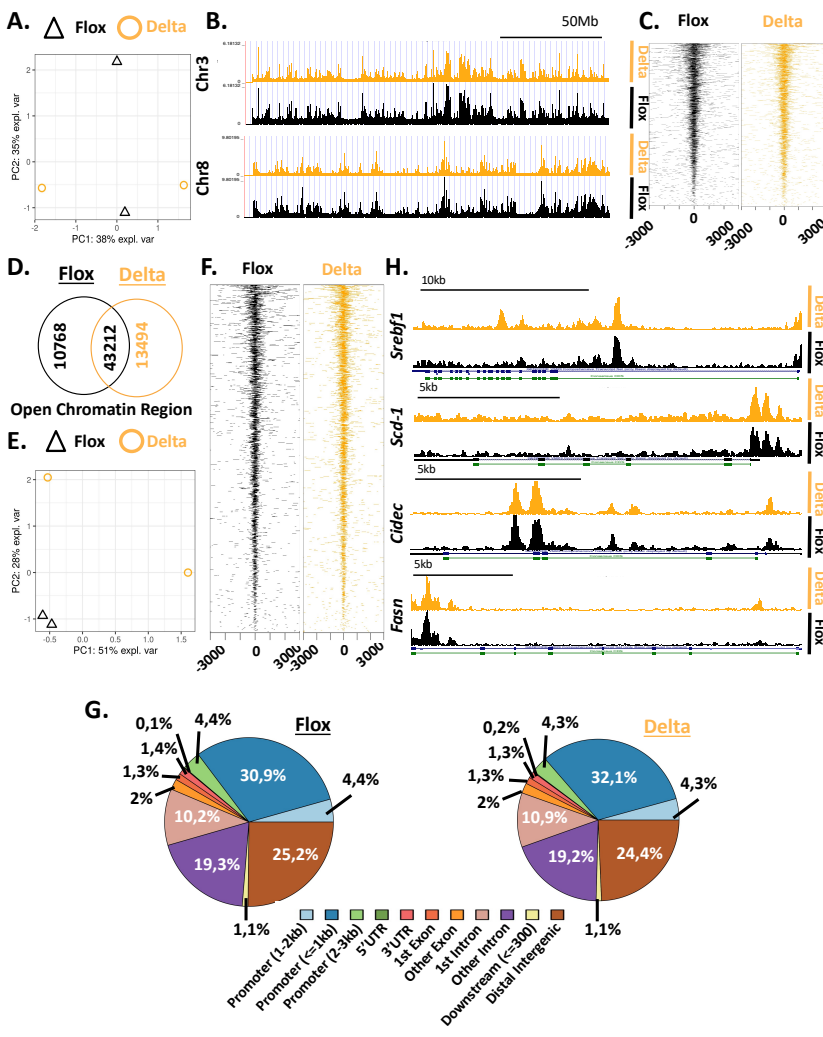


Fig. S8. Hepatocyte specific *Hmgb1* deletion does not remodel chromatin.

(A) Principal component analysis scores plot of ATAC-seq data of liver tissue from HMGB1^{fl/fl} (black triangle, n=2) and HMGB1^{ΔHep} (orange circle, n=2)) mice on chow diet. (B) UCSC genome browser of tracks showing HMGB1 similar chromatin open region in Chromosome 3 and 8. (C) Average coverage around TSS in liver biopsies of HMGB1^{fl/fl} (black) and HMGB1^{ΔHep} (orange) mice. (D) Venn Diagram showing overlapping opened region and and (E) Principal component analysis scores plot of ATAC-seq data of liver tissue from HMGB1^{fl/fl} (black triangle, n=2) and HMGB1^{ΔHep} (orange circle, n=2) mice subjected to F/R. (F) Average coverage around TSS in liver biopsies of HMGB1^{fl/fl} (black) and HMGB1^{ΔHep} (orange) mice after F/R challenge. (G) Chart pie displaying the genomic distribution of open chromatin domain in liver biopsies from HMGB1^{fl/fl} (black, n=2) and HMGB1^{ΔHep} (orange, n=2) mice. (H) UCSC genome browser snapshots of tracks showing HMGB1 chromatin open region of canonical LXRx and PPAR γ responsive gene loci (*Srebfl*, *Scd-1*, *Cidec*, *Fasn*) in liver biopsies of HMGB1^{fl/fl} (black) and HMGB1^{ΔHep} (orange) mice after F/R challenge.

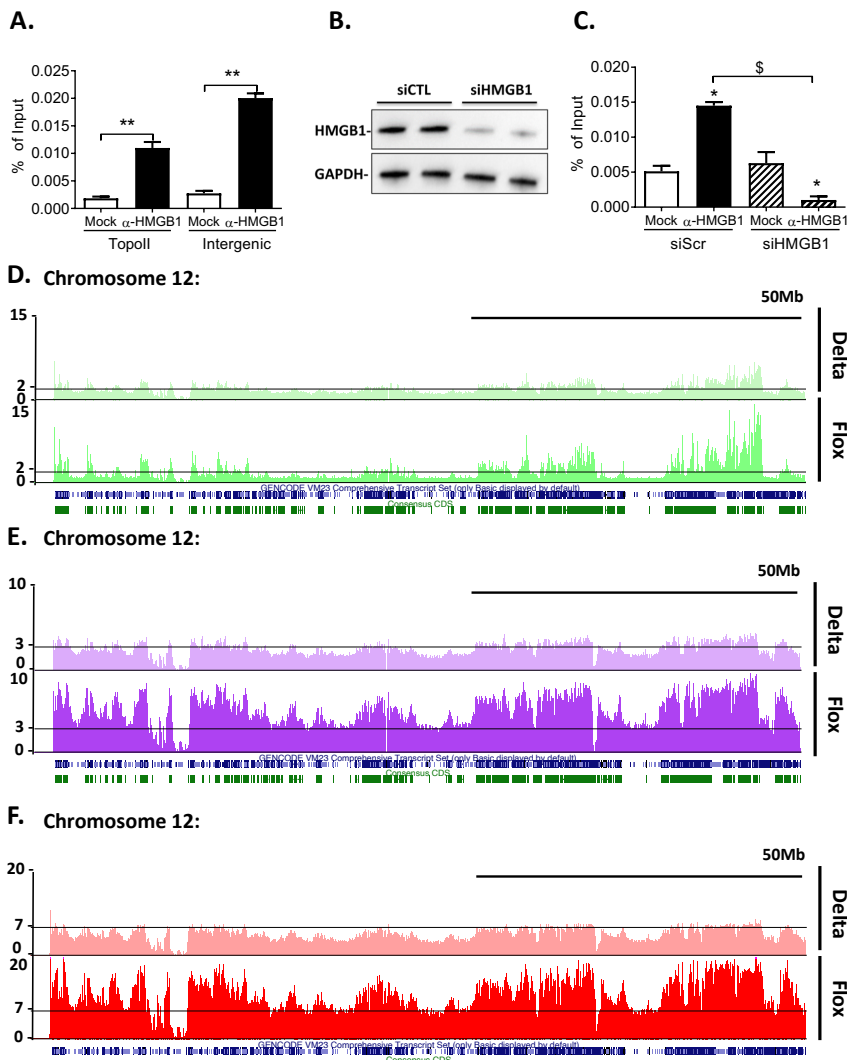


Fig. S9. Validation of HMGB1 ChIP *in vitro* and *in vivo*.

(A) Chromatin immuno-precipitation was performed against HMGB1 on U2OS cells and enrichment on TOPO isomerase II promoter sequence as well as intergenic region were measured by RT-qPCR. (B-C) To validate specificity of the ChIP, (B) U2OS cells were first transfected with a siRNA targeting HMGB1 and after successful knockdown of HMGB1 showed by immunoblot targeting HMGB1 with GAPDH as a loading control, (C) ChIP experiment has been conducted, and siHMGB1 treated cells showed no DNA enrichment of TOPOII promoter region while siScramble exhibits a significant DNA enrichment. (D-F) UCSC genome browser of tracks from the ChIP-seq data, comparing the sequencing signal in Chromosome 2 from HMGB1^{fl/fl} ($n=2$) and HMGB1^{ΔHep} ($n=2$) mice upon (D) Chow diet (green), (E) HFD (purple) and (F) F/R (red). Data are means \pm SEM of three independent experiments (A-C) * $p<0.05$ ** $p<0.01$ α HMGB1 vs Mock, \$<0.05\$ siScramble vs siHMGB1 by unpaired Mann and Whitney comparison or two-way ANOVA

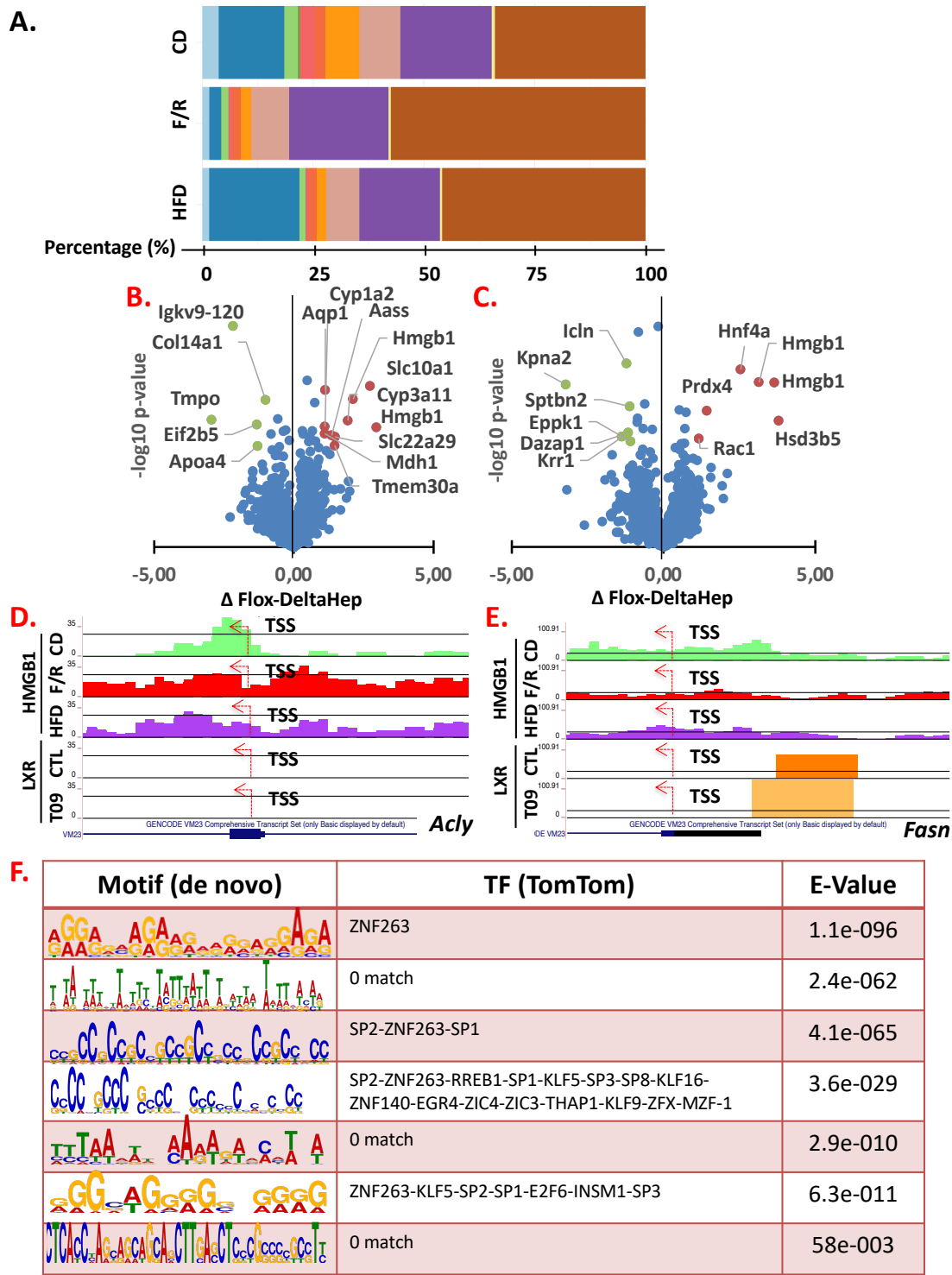


Fig. S10. Genomic distribution and proteomic analyses of HMGB1.

(A) Genomic distributions of enriched regions identified in ChIP-seq data sets in liver biopsies of HMGB1^{fl/fl} mice subjected to chow diet, HFD and F/R. (B-C) Volcano plots of proteins identified to be associated with HMGB1 in liver nuclear extracts of mice (n=4) subjected to HFD (B) or after F/R (C). (D-E) UCSC genome browser shot of HMGB1 and LXRx ChIP-seq data along the locus of *Acly* (D) and *Fasn* (E) gene loci. HMGB1 tracks in liver from HMGB1^{fl/fl} upon chow diet (green), after F/R (red) and HFD (purple). LXRx tracks from basal liver (dark orange) and T09 challenged liver (light orange). Coverage on gene locus and TSS region (-1kb/+1kb) of LXRx responsive gene: *Acly* (D) and *Fasn* (E). Exon 1 model (blue) is displayed on the bottom track. (F) Table of significant *de novo* motifs identified, using the MEME Suite, across the HMGB1 ChIP peaks in the promoter region (+/-3kb) flanking the TSS of 134 genes belonging to the metabolism GO term.

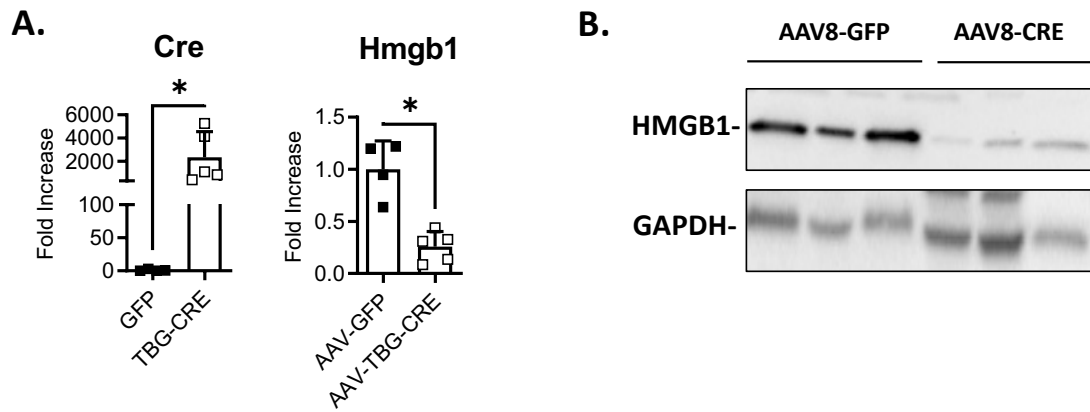


Fig. S11. Successful *in vivo* knockdown of *Hmgb1* gene and protein using AAV-TBG-Cre.

Adult $\text{HMGB1}^{\text{fl/fl}}$ mice were infected either with AAV8-Gfp (n=3) or AAV8-Tbg-Cre (n=3) to selectively generate *Hmgb1* deletion in hepatocytes *in vivo*. (A) The level of expression of *Hmgb1* gene was determined using RT-qPCR in whole liver. (B) Representative immunoblot targeting HMGB1 in liver extracts. GAPDH was used as a loading control. Data are means \pm SEM. *p<0.05, **p<0.01, ***p<0.001, ****p<0.0001 by unpaired Mann and Whitney comparison.

Table S1. List of genes highly occupied by HMGB1 in Chow Diet compare to HFD

GO « Integration of Energy Metabolism »	GO « Phospholipid Metabolism »
Abcc8	Acp6
Acaca	Agpat1
Acacb	Agpat5
Acly	Arf1
Acsl3	Awat2
Adcy5	Cds2
Adipor2	Cept1
Adra2c	Cpne1
Cacna1a	Cpne3
Cacna1c	Cpne7
Cacna2d2	Ddhd2
Cacnb2	Enpp6
CD36	Etnk1
Fasn	Gnpat
Gcg	Gpat2
Gcgr	Gpat3
Glp1r	Gpat4
Gna11	Hadha
Gna14	Inpp4b
Gna15	Inpp5f
Gnai1	Liph
Gnai2	Lpcat2
Gnaq	Lpcat3
Gnas	Lpin3
Gnb1	Mfsd2a
Gnb2	Mgll
Gnb3	Miga1
Gng11	Mtm1
Gng12	Mtmmr14
Gng13	Mtmmr7
Gng3	Osbpl10
Gng5	Osbpl5
Gng8	Osbpl8
Itpr1	Phospho1
Itpr2	Pik3ca
Itpr3	Pik3cd
Kcnb1	Pik3r2
Kcnc2	Pik3r3
Kcng2	Pip5k1a
Kcnj11	Pip5k1b
Marcks	Pitpnrb
Mlx	Pitpnrm2

Mlxip1	Pla2g12a
Plcb1	Pla2g15
Plcb2	Pla2g1b
Plcb3	Pla2g2d
Prkag2	Pla2g2e
Prkar1a	Pla2g4d
Prkar1b	Pla2g4f
Prkca	Pla2g5
Rapgef4	Plb1
Slc2a1	Plekha1
	Plekha2
	Plekha5
	Pnpla6
	Pnpla8
	Ptpn13
	Rab4a
	Selenoi
	Slc44a1
	Slc44a2
	Slc44a3
	Slc44a5
	Stard10
	Stard7
	Taz
	Tnfaip8l1
	Tnfaip8l2
	Tnfaip8l3
	Tpte
	Vac14

Table S2. List of genes highly occupied by HMGB1 in Chow Diet compare to F/R

GO « Integration of Energy Metabolism »	GO « Phospholipid Metabolism »
Acaca	Acp6
Acacb	Agpat1
Acly	Agpat5
Acsl3	Arf1
Acsl4	Awat2
Adcy5	Cds2
Adcy6	Cept1
Adipor2	Cpne1
Adra2c	Cpne3
Agpat1	Cpne7
Cacna1a	Ddhd2
Cacna1c	Enpp6
Cacna2d2	Etnk1
Cacnb2	Gnpat
Cacnb3	Gpat2
Cd36	Gpat3
Fasn	Gpat4
Gcg	Hadha
Gcgr	Inpp4b
Glp1r	Inpp5f
Gna11	Liph
Gna14	Lpcat2
Gna15	Lpcat3
Gnai1	Lpin3
Gnai2	Mfsd2a
Gnaq	Mgll
Gnas	Miga1
Gnb1	Mtm1
Gnb2	Mtmr14
Gnb3	Mtmr7
Gng10	Osbpl10
Gng11	Osbpl5
Gng12	Osbpl8
Gng13	Phospho1
Gng3	Pik3ca
Gng5	Pik3cd
Itpr1	Pik3r2
Itpr2	Pik3r3
Itpr3	Pip5k1a
Kcnb1	Pip5k1b
Kcnc2	Pitpn
Kcng2	Pitpn
Kcns3	Pla2g12a
Marcks	Pla2g15
Mlx	Pla2g1b

Mlxip1	Pla2g2d
Plcb1	Pla2g2e
Plcb2	Pla2g4d
Plcb3	Pla2g4e
Prkab2	Pla2g4f
Prkaca	Pla2g5
Prkag2	Plb1
Prkar1a	Plekha1
Prkar1b	Plekha2
Prkar2b	Plekha5
Prkca	Pnpla6
Rap1a	Pnpla8
Rapgef3	Ptpn13
Rapgef4	Rab4a
Slc2a1	Selenoi
	Slc44a1
	Slc44a2
	Slc44a3
	Slc44a5
	Stard10
	Stard7
	Taz
	Tnfaip8l1
	Tnfaip8l2
	Tnfaip8l3
	Tpte
	Vac14

Table S3. Primers for Real time qPCR

Gene	Forward Primer	Reverse Primer
36B4	AGTCGGAGGAATCAGATGACGAT	GGCTGACTTGGTTGCTTG
Abcg5	TCGCAACGGTCATTTC	GCCAAAAGAGCAGCAGAGAAATA
Abcg8	GCGTCTGTCGATGCTGGTC	ATCCATTGGCCACCCTGT
Acc1	CTCCTTGCCTCCGACATC	TACCATGCCAATCTCATTCCTC

<i>Acc2</i>	TGGAGGCAACAGGGTCATAGA	CGCAGCGATGCCATTGT
<i>Acly</i>	AAAGCTTGGCCTCGTCGG	GGGACGAAGGGTTCAATGAGA
<i>Adrp47</i>	GTGTCGTCGTAGCCGATGC	CCATTCTCAGCTCCACTCCAC
<i>Agk</i>	GTGTTGGCAACCAGCTATT	GCTGCGGGATTGAGAAAGAC
<i>Fabp4</i>	TTCGATGAAATACCGCAGA	GGTCGACTTCCATCCCACCT
<i>Cd11b</i>	TCGGACGAGTCCGGATT	TGTGATCTGGCTAGGGTTTC
<i>Cd11c</i>	GATTCAGCATCCCAGATCCC	CCAGATCCACCAAGTCCATCC
<i>Cd36</i>	GGACATACTTAGATGTGAAACCCATA	TGTTGACCTGCAGTCGTTTG
<i>Cd45</i>	ACATGCTGCCAATGGTCTG	GTCCCACATGACTCCTTCCTATG
<i>Chrebp</i>	ACATCAGCGCTTGACCAGAT	TGCGCGTCCGGACATAG
<i>Cidec</i>	GACTTATTGGCTGCCTGAACG	ATCTCCTCACGATGCGCTT
<i>Cpt1a</i>	CACCAACGGGCTCATCTTCT	CCTCTATGAATTGCTCTGGTT
<i>Cpt1b</i>	GTGCAAGCAGCCGTCTAG	TTGCGGCGATACATGATCA
<i>Cre</i>	CATTGCTGTCACTTGGTCGT	CATTGGGCCAGCTAACAT
<i>Cyp4a14</i>	TCAGTCTATTCTGGTGCTGTT	GAGCTCGTTGCCTTCAGATGGT
<i>Elov16</i>	TCTGATGAACAAGCGAGCCA	TGGTCATCAGAATGTACAGCATGT
<i>F4/80</i>	TGACAACCAGACGGCTTGTG	GCAGGCGAGGAAAAGATAGTGT
<i>Fasn</i>	ATCCTGGAACGAGAACACGATCT	AGAGACGTGTCACTCCTGGACTT
<i>Fgf21</i>	GGTCAAGTCCGGCAGAGGTA	CTGTTCCATCCTCCCTGATCTC
<i>G6pc</i>	ACGTATGGATTCCGGTGTGTTG	CAGCTGCACAGCCCAGAA
<i>Gck</i>	TCGCAGGTGGAGAGCGA	TCGCAGTCGGCGACAGA
<i>Gk</i>	GTGTTGGCAACCAGCTATT	GCTGCGGGATTGAGAAAGAC
<i>Gys1</i>	CGGCTTGGCTGCTTATG	CCAGAATGAAATGCCGTAAGCT
<i>Gys2</i>	CCAACGACGGATGGCTTAA	GATCCTGACGGAGAAGGTGGTA
<i>Hk2</i>	CGCCGGATTGGAACAGAA	CCCGTCGCTAACTCACTCACT
<i>Hmgb1</i>	AGCCCTGTCCTGGTGGTATT	CCAGGCAAGGTTAGTGGCTA
<i>Hmgcr</i>	TTGTTCACGCTCATAGTCGCT	GACACATCTCGTCCAGACCC
<i>L-pk</i>	AGTCGTGCAATGTTCATCCCT	TCGACTCAGAGCCTGTGGC
<i>Ldl-r</i>	TGGATCCACCGCAACATCTA	CTCTTACGCCCTGGTGTCA
<i>Lpl</i>	TTATCCAATGGAGGCACTTTC	CACGTCTCCGAGTCCTCTCT
<i>Lxra</i>	AGGAGTGTGACTTCGCAA	CTCTTCTGCCGCTTCAGTT
<i>Lxrbeta</i>	AAGCAGGTGCCAGGGTTCT	TGCATTCTGTCCTGTGGTTGT
<i>Pck1</i>	ATGTTGGCGGATTGAAG	TCAGGTTCAAGGCCTTCC
<i>Pnpla2</i>	CGCCTCTCGAAGGCTCTTT	TGTAGCCCTGTTGCACATCTC
<i>Pnpla3</i>	AGCCCGTCTGATGCACTT	ACGCGGTACCTCGTGT
<i>Ppara</i>	TGGCAGCAATATCAGAGGTAGATT	ATCATATCAAAGGAGCTGCCAA
<i>Pparg (Fluidigm)</i>	CCGAAGAACCATCCGATTGA	TTTGTGGATCCGGCAGTTAAG
<i>Pparg (LKO)</i>	GATGCACTGCCATTGAGCACTT	GAATGGCATCTCTGTGTCAACC
<i>Pparg1ca</i>	AAAGGATGCGCTCTGTTCA	GGAATATGGTGATCGGAACA
<i>Ppargc1b</i>	TTGAGGTGTTCCGGTGAGATTGTAG	GAAGGGTATAAAACCGTGCTTCTG
<i>Pygl</i>	CAAGTGTCCAAGAGGGTGT	TGTAATGTTGGCCATGT
<i>Scd-1</i>	CAACACCATTGGCGTTCCA	GGTGGGCGCGGTGAT

<i>Serp2</i>	CAACACAGGGATCCAGGTCT	CATGAGGCCGTGACTTGATG
<i>Sqle</i>	CTGCACTTGGTTGGTTCTGAC	GGAGGGCTACCGTGTCTCCA
<i>Srebf1</i>	CTGGCTTGGTGATGCTATGTTG	GACCATCAAGGCCCCCAA
<i>Tfam</i>	GCACCCCTGCAGAGTGTCAA	CGCCCAGGCCTTACCTT
<i>Tip47</i>	GGCTGGACAGACTGCAGGA	TCTTGAGCCCCAGACACTGTAG
<i>Ucp2</i>	CCTCAAAGCAGCCTCCAGAA	TCAATCGGCAAGACGAGACA
<i>Vnn1</i>	ATGAGGTTATGCCTTGGAGC	CCACAGGTGCGTAAATTGGTAG